Blending Different Fineness Cements to Engineer the Properties of Cement-Based Materials

Dale P. Bentz
Building and Fire Research Laboratory
National Institute of Standards and Technology
100 Bureau Drive Stop 8615
Gaithersburg, MD 20899-8615 USA
Phone: (301)975-5865
Fax: (301)990-6891
E-mail: dale.bentz@nist.gov

Abstract

Concretes are designed to fulfill specific engineering requirements, most commonly exemplified by slump, unit weight, and compressive strength. One source of untapped potential for varying engineering properties of hardened concrete is the variation of the cement particle size distribution. In this study, the performance of cements prepared by blending a coarse ASTM C150 Type I/II and a fine Type III cement obtained from the same clinker in three different proportions is examined. Evaluated properties for pastes and mortars include isothermal and semi-adiabatic calorimetry, chemical shrinkage, setting times (Vicat needle), compressive strength, and autogenous deformation. Addition of a high range water reducer to the Type III cement and the two finest blends is investigated as a secondary variable. The properties of the blends are compared to those of the two pure starting materials using a law of mixtures. Some properties such as heat release (as assessed using isothermal calorimetry) and chemical shrinkage are predicted nearly perfectly by applying this simple law. Others such as peak temperature (as assessed using semi-adiabatic calorimetry) and compressive strength are adequately predicted for engineering purposes by application of the law. Finally, setting times and autogenous deformation, being dependent on both hydration rates and particle spacing, can not be predicted by the simple law of mixtures. It is concluded that a wide range of performance properties can be achieved by the blending of a fine and a coarse cement in controlled proportions.

Keywords: Blending; fineness; hydration; particle size distribution; strength.

Introduction

Most concrete specifications include a requirement for the 28-day compressive strength. Due to inherent variability in field placement conditions (weather, location, micro-environment), concretes are generally designed to exceed the specified 28-day strength value by some safety margin (perhaps 10 % or more). As each ready-mix plant typically only stocks one (or perhaps two) cements at a given time, strength adjustments are usually performed on the basis of changing the water-to-cement ratio (*w/c*) of the concrete, adjusting the cement (paste) content, the addition of specific chemical admixtures, or some combination of these approaches. However, such mixture modifications will also influence the transport properties and potentially the durability of the in-place concrete. Thus, in some cases, it would be desirable to adjust the

28-d strength of a concrete without changing any of these three parameters, or at a specific constant water content, for example.

These current practices for adjusting 28-d strength essentially ignore the inherent and strong linkage between cement particle size distribution (PSD) and compressive strength.[1-3] Osbaeck and Johansen[2] have established that the complete cement PSD must be utilized when correlating strength development to fineness (as opposed to a single number such as Blaine fineness) and further demonstrated that the influence of PSD on strength could be captured adequately using a mathematical model that assumes that the depth of reaction (from the particle surface) for each particle is only a function of time. Wakasugi et al.[3] have suggested that adjusting the fineness of a belite-based cement provides the possibility to manufacture concrete with (various) requisite properties. Extending on these findings, this paper explores the possibility of engineering properties by the controlled blending of a fine and a coarse cement obtained from the same clinker. Practically, this would require that the ready-mix plant maintain two silos of cement, one for each fineness. Seasonal or other strength adjustments could then be obtained by the controlled blending of the cements from these two silos.

Research Significance

Concrete ready-mix producers are faced with the challenging task of providing a product with consistent properties despite the fact that field conditions are highly variable. Traffic and the weather remain two variable entities, and both can dramatically influence the properties developed by the concrete after it leaves the ready-mix plant. Seasonal and other adjustments to mixture proportions are often accomplished via the judicious addition of chemical admixtures. Although not employed in current practice, an alternative approach to engineering concrete performance can be via the adjustment of the PSD of the cement powder. As a first step in reducing this concept to practice, this paper demonstrates the blending of a fine ASTM C150[4] Type III cement and a coarse Type I/II cement produced from the same clinker to produce cement pastes and mortars with a wide range of compressive strengths and other engineering properties. The Blaine finesses of the coarse (302 m^2/kg) and fine (643 m^2/kg) cements employed in this study can be contrasted against those of Type I/II cements, whose typical fineness values have increased from about 330 m^2/kg in the 1950s to about 400 m^2/kg currently.[5]

Experimental

Materials and Mixture Proportions

Three cements produced from the same clinker but of widely different finenesses were obtained from a U.S. cement plant. Blaine finenesses and oxide compositions, as provided on mill sheets for the three, are summarized in Table 1. Each cement has been separately optimized for sulfate, with the calcium sulfate content (as indicated by SO_3 in Table 1) increasing with cement fineness, as would be expected. Measured differential particle size distributions for the three cements are provided in Figure 1. PSD measurements were performed using a "wet" laser diffraction technique with isopropanol as the suspension media.

Three blends were prepared from the Type I/II and Type III cements. Specifically, blends with mass proportions of 25:75, 50:50, and 75:25 were homogenized in 1000 g batches by mixing for 30 min in a sealed plastic jar on a Turbula[A] blender. The measured PSDs for the three blends are given in Figure 1. As shown in the lower left of Figure 1, the 50:50 blend has a PSD that is fairly similar to that of the Type II/V cement and will provide an interesting contrast as it and the Type II/V cement will have similar bulk chemical composition and overall PSDs, but likely different PSDs for their calcium sulfate fractions which have experienced different grinding conditions. In general, there is good agreement between the PSD measured for each blend and that calculated by applying a law of mixtures to the measured PSDs for the two component cements. The law of mixtures for a two-component blend is given by:

$$P(\text{blend}) = P(\text{component 1})*\text{mass fraction (1)} + P(\text{component 2})*\text{mass fraction (2)} \quad (1)$$

where P is the property of interest (differential volume fraction of particles, strength, heat release, chemical shrinkage, etc.).

Table 1. Fineness and Oxide Compositions of the Three Cements (from the Same Clinker)

	Type I/II Coarse	**Type II/V**	**Type III**
Blaine fineness (m^2/kg)	302	387	613
SiO_2	20.7	21.1	20.7
Al_2O_3	4.5	4.5	4.5
Fe_2O_3	4.1	4.1	4.1
CaO	64.4	64.9	64.8
MgO	1.1	1.2	1.2
SO_3	2.2	2.5	2.8
LOI	1.1	1.3	1.3
Alkalis (Na_2O equiv.)	0.30	0.31	0.32

For this study, a single water-to-cement ratio (*w/c*) of 0.40 by mass was employed. Both cement pastes and mortars (Table 2) were prepared, the former in a high shear blender and the latter in a planetary mixer. To assure adequate workability, a high range water reducer (HRWRA) was used for the mortars prepared with the Type III cement and with the 50:50 and 25:75 blends. Actually, for the 50:50 blend, mortars were prepared both with and without the HRWRA to examine its influence on measured properties. For the mortar prepared with the Type III cement, the HRWRA was added at a dosage of 0.67 % by mass of cement, within the dosage range suggested by the HRWRA manufacturer. This dosage was reduced proportionally for the 25:75 and 50:50 blends to 0.5 % and 0.33 %, respectively. The measured air contents of the mortars ranged from 1 % to 3 %.

[A] Certain commercial products are identified in this paper to specify the materials used and procedures employed. In no case does such identification imply endorsement or recommendation by the National Institute of Standards and Technology, nor does it indicate that the products are necessarily the best available for the purpose.

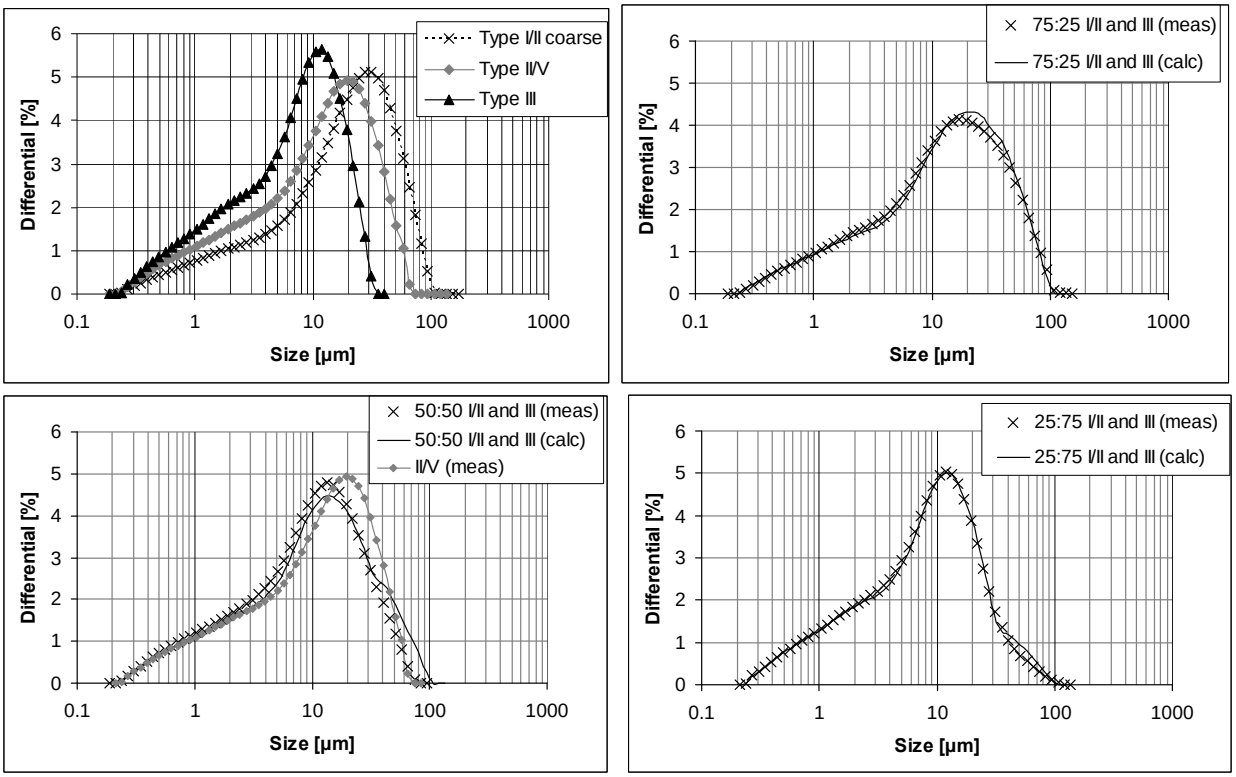

Figure 1. Measured (via laser diffraction) and calculated particle size distributions for three original cements (top left) and for the three different blends of the Type I/II (coarse) cement with the Type III (fine) one. The shown results are the average of six individual measurements and the error bars (one standard deviation) would fall within the size of the shown symbols. (One micrometer is equivalent to 3.9 x10^{-5} in.)

Table 2. Mixture Proportions for Mortars Examined in Study

Ingredient	Mass
Cement	1250.0 g (2.75 lb)
Water	500.0 g (1.10 lb)
F95 fine sand[B]	700.6 g (1.54 lb)
Graded sand (ASTM C778[6])	532.5 g (1.17 lb)
20-30 sand (ASTM C778[6])	532.5 g (1.17 lb)
S16 coarse sand[B]	1036.9 g (2.28 lb)

[B]F95 and GS16 correspond to sand supplier designations.

Measurements

The following measurements were conducted on the cement paste and mortar specimens: 1) Isothermal calorimetry – the heat of hydration was measured during the course of 7 d of sealed curing on 5 g (0.18 oz) samples of pre-mixed cement pastes or 7.45 g (0.26 oz.) samples of pre-mixed mortars using a TAM Air Calorimeter[A] at 25 ºC; to provide an indication of variability, two specimens were evaluated for each cement paste or mortar,
2) Semi-adiabatic calorimetry – the semi-adiabatic temperature rise was measured during the course of 3 d on single sealed cement paste or mortar specimens with a mass of approximately

330 g (0.73 lb) using a custom-built semi-adiabatic calorimeter unit;[5,7] replicate specimens have indicated a standard deviation of 1.4 °C (2.5 ºF) in the maximum specimen temperature achieved during a 3 d test,[5]
3) Chemical shrinkage – measured during the course of 7 d on triplicate saturated cement paste specimens, using the ASTM C 1608 standard test method at 25 ºC;[8] according to the ASTM standard, the expected single laboratory precision for the test is 0.0042 kg of water per kg of cement (lb of water per lb of cement),
4) Time of setting – measured on duplicate cement paste specimens based on penetration of the Vicat needle according to ASTM C 191;[9] in the standard, the single laboratory precisions for pastes prepared at normal consistency are listed as 12 min and 20 min for initial and final times of setting, respectively,
5) Compressive strength – measured at 1 d, 3 d, 7 d, 28 d, and 90 d to 92 d on mortar cube specimens cured in a saturated solution of calcium hydroxide, according to the procedures in ASTM C 109,[10] but with a loading rate of 20.7 MPa/min (3000 psi/min), switching to deformation control once a stress of 13.8 MPa (2000 psi) was reached; three specimens were evaluated at each time, with the averages and standard deviations being provided in the results to follow,
6) Autogenous deformation – measured on triplicate mortar specimens sealed in corrugated tubes[11] (procedure is currently being standardized in ASTM subcommittee C09.68); in the draft standard, the single laboratory precision is listed as 30 microstrains for mortar specimens.

Modeling

It is well established that the cement PSD has a large influence on the interparticle spacing in the fresh cement paste and also on the (reactive) surface area. For the cements investigated in this study, simulations of the initial three-dimensional microstructures have been conducted using previously developed software.[12] A three-dimensional computational cube of dimension 200 μm (0.0078 in) on a side is employed and the cement particles are modeled as impenetrable spheres that follow the measured PSDs (as provided in Figure 1). The particles are placed from largest to smallest at random locations within the three-dimensional computational volume, such that no overlaps occur. Simulation results are summarized in Figure 2 that provides graphs of the volume fraction of the total water that is within a given distance of a cement particle surface, respectively. This measure has previously been related to the size of the pores that will first empty during self-desiccation in the hydrating cement paste.[12] As fineness increases, the reactive surface area increases, while the interparticle spacing decreases. Both of these changes will influence a variety of properties including hydration, setting, strength development, and autogenous deformation, as will be explored throughout the remainder of this paper.

In Figure 2, an attempt has been made to apply the law of mixtures (equation 1) to the three cement blends to predict the volume fraction vs. distance curves based on the curves obtained for the pure Type I/II and Type III cements. It can be seen that while capturing the general trend in the curves, the predictions based on the law of mixtures are not able to match the values obtained on the simulated three-dimensional microstructures, particularly for the larger distance values that are of importance for estimating the sizes of the pores that will first be emptied during self-desiccation.[12] It should be kept in mind that the simulations for Figure 3

were conducted with a **random** placement of the cement particles, as opposed to the flocculation and/or dispersion that commonly occur to various extents in the actual paste and mortar mixtures (with and without an HRWRA).

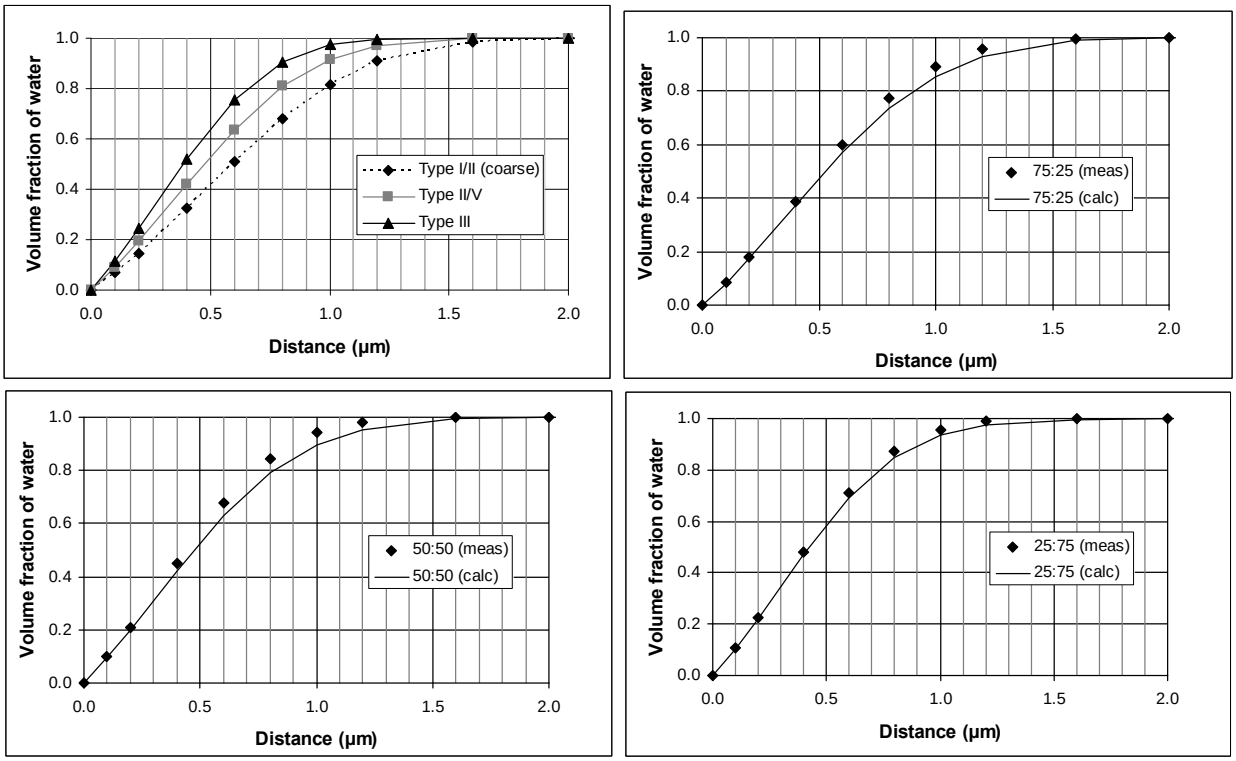

Figure 2. Volume fraction of water within a given distance of a cement particle surface for the simulated initial cement microstructures for *w/c* = 0.4 cement pastes. (One micrometer is equivalent to 3.9 x10^{-5} in.)

Results and Discussion

Cement Pastes

Isothermal Calorimetry

Figure 3 provides plots of the heat release rate (heat flow) for the first 24 h of hydration for the six cement pastes examined in this study (3 pure and 3 blends). In general, results for the two replicate specimens for each cement paste fall directly on top of one another. For the three initial cements, the heat release during the first 24 h increases with increasing cement fineness, as would be expected due to the increased (in contact with water) surface area. Interestingly, for these six cements based on a single clinker, the peak in heat release rate always occurs at about 6 h, while by 24 h, the heat release rate has diminished to a value close to 0.001 W/g cement (1.548 Btu/lb cement). In 1950, Verbeck and Foster, based on a compiled data set for cements of that time period with Blaine fineness between 285 m^2/kg and 490 m^2/kg, estimated that an increase in Blaine fineness from 300 m^2/kg to 400 m^2/kg should increase 7-day heat of hydration by about 40 J/g.[13] For the Type I/II and Type II/V cements investigated in this study, going from 302 m^2/kg to 387 m^2/kg increases the 7-day heat release from 298.9 J/g to 345.3 J/g (Figure 5),

for an estimated increase of 54.6 J/g per 100 Blaine fineness units, significantly higher than the Verbeck and Foster value. One reason for this increased value could be the generally increased C_3S and C_3A contents of current cements relative to those of 1950, as these two phases are the most reactive at early ages and exhibit highly exothermic hydration reactions.

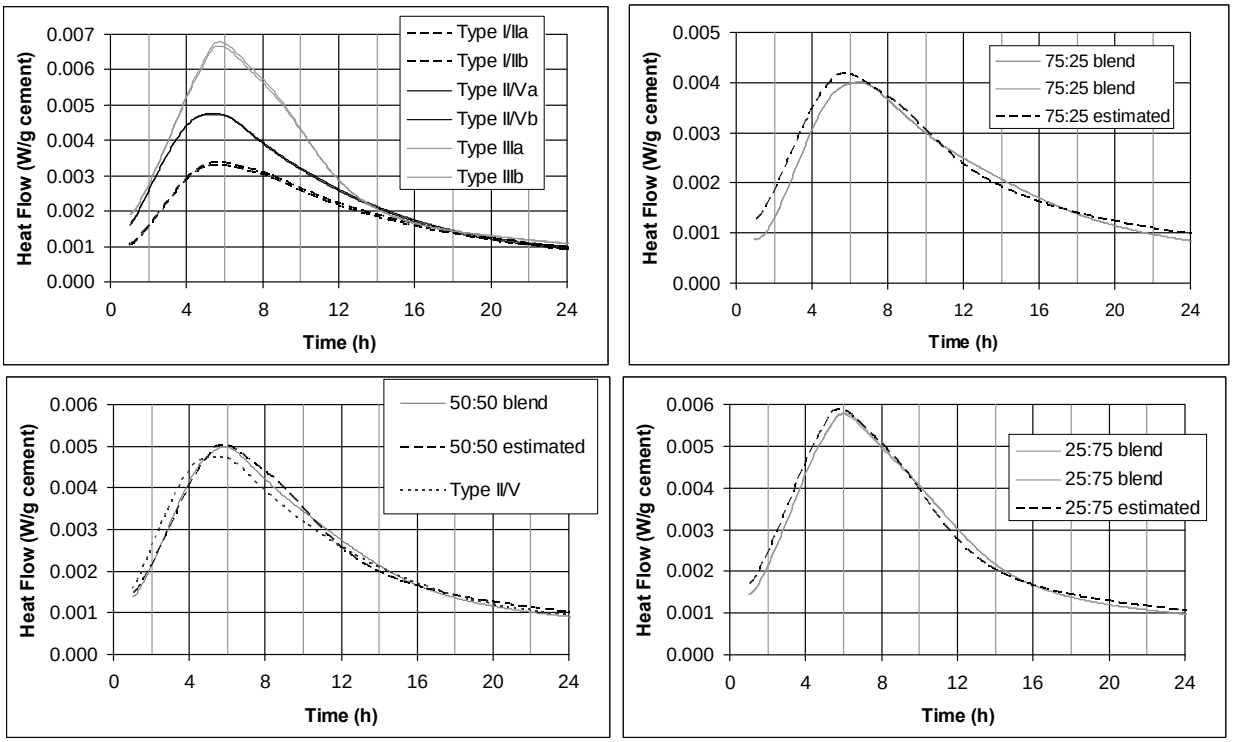

Figure 3. Isothermal calorimetry results out to 24 h for Type I/II, II/V, and III cements (top left) and for the three blends (*w/c* = 0.4 pastes). Results for two replicate specimens are shown for most pastes. 1 W/g = 1548 Btu/(h·lb).

The heat flows measured during the first 24 h for the three blended cements are predicted quite well by applying the simple law of mixtures. While some minor discrepancies between these predictions and the experimental data are observed, the predictions basically qualitatively and quantitatively agree with their experimental counterparts. These results imply that for the *w/c* = 0.4 cement pastes examined in this study, the particles are likely hydrating independently of one another during the first 24 h, such that the degree of hydration of blends of the fine and coarse cements can be quite accurately computed simply as a weighted average of their (measured) individual hydration rates. In the lower left graph of Figure 3, it can also be noted that the 50:50 blend exhibits an isothermal heat flow curve during the first 24 h of sealed curing that is quite similar to that of the original Type II/V cement, which has a similar PSD (Figure 1).

The influence of the HRWRA on initial heat release rates of the Type III *w/c* = 0.4 cement paste is provided in Figure 4, where it is observed that the HRWRA produces a small but measurable retardation of 1 h or less, during the first 24 h of hydration. The similarity of these heat release curves will be contrasted both against the setting time behavior of these four cement pastes and the influence of HRWRA on cement hydration in mortars, in the results to follow.

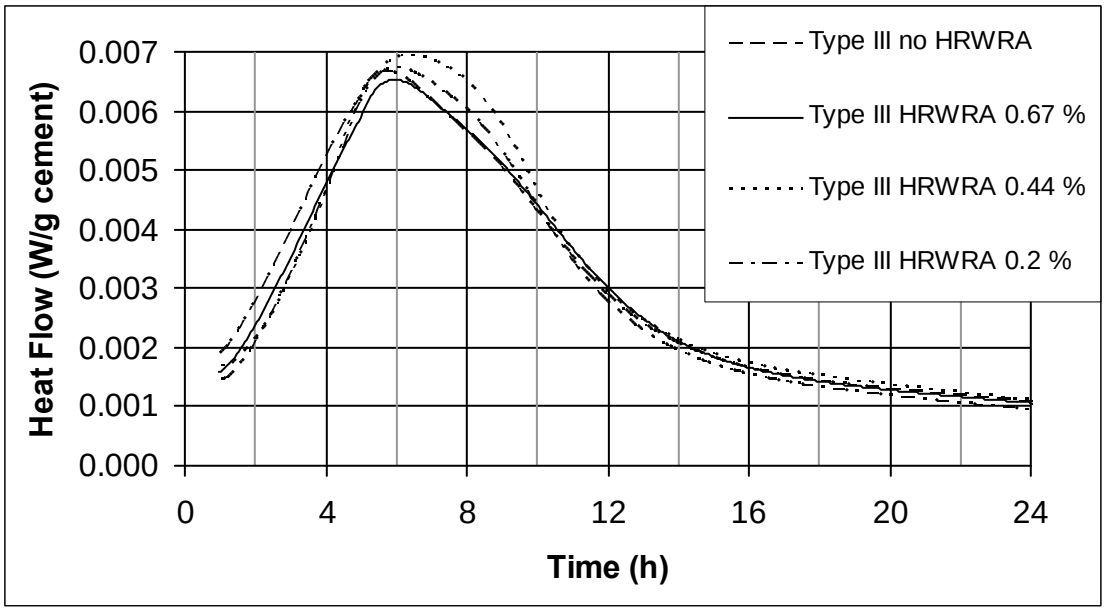

Figure 4. Isothermal calorimetry results out to 24 h for Type III *w/c* = 0.4 cement pastes with various addition rates (by mass of cement) of HRWRA. 1 W/g = 1548 Btu/(h·lb).

Chemical Shrinkage

Chemical shrinkage provides an alternate measure of degree of hydration of cement-based materials. In 1935, Powers[14] demonstrated a direct proportionality between heat of hydration and chemical shrinkage, using a scaling factor of 80.8 (J/g)/(g water per 100 g cement) or 34.74 (Btu/lb)/ (lb water per 100 lb cement) to convert from chemical shrinkage to heat release, for four different cements of that era. The results in Figure 5 demonstrate that for the three initial cements produced from the same clinker, a direct proportionality is observed once again between these two measures of hydration, here with a scaling factor of 80. (J/g)/(g water per 100 g cement) or 34.4 (Btu/lb)/(lb water per 100 lb cement), almost identical to the value found by Powers. This nearly exact agreement in factors, however, is only coincidental, as factors ranging from about 65 (J/g)/(g water per 100 g cement) to about 85 (J/g)/(g water per 100 g cement) have been found for other cements, although in each case a direct proportionality was observed.[5,15]

Since chemical shrinkage and heat release provide "equivalent" measures of hydration and it has been shown earlier that the law of mixtures applies quite well to the heat release curves, it is not surprising that it works equally well for predicting the chemical shrinkage of the cement blends, as exemplified by the results shown in Figure 6 for the 75:25 blend of the Type I/II and Type III cements.

Semi-adiabatic Calorimetry

The measured semi-adiabatic temperature curves are provided in Figure 7 and the maximum temperature obtained in each experiment and the time when this maximum is achieved are provided in Tables 3 and 4, respectively. As cement fineness is increased, it is noted that the maximum temperature increases and occurs up to about three hours earlier. Both the maximum

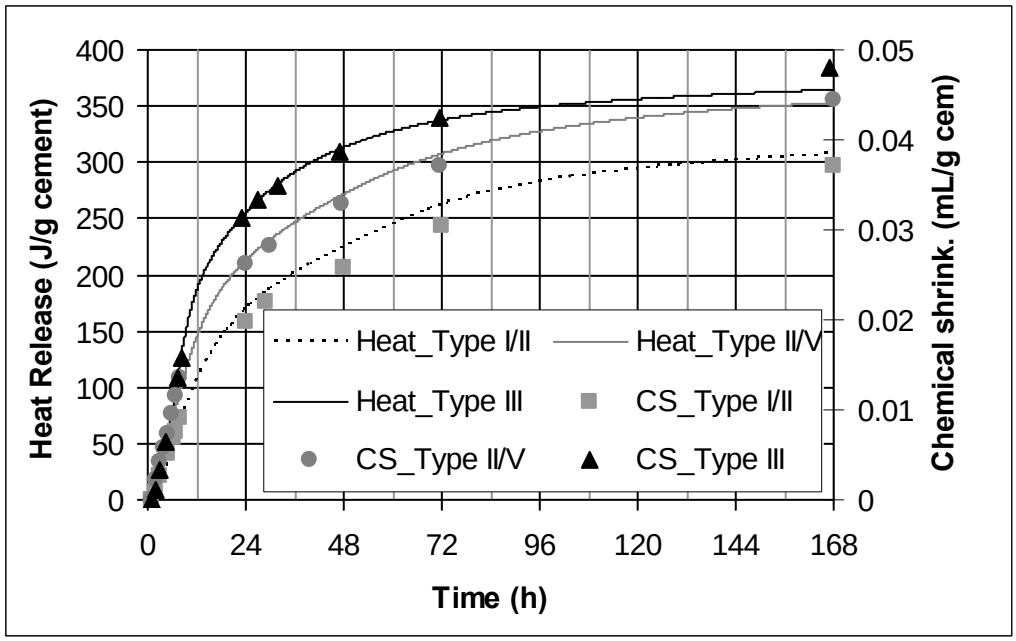

Figure 5. Comparison of measured isothermal calorimetry cumulative heat release and chemical shrinkage (CS) for the three initial cements (Types I/II, II/V, and III). 1 J/g = 0.43 Btu/lb and 1 mL/g = 15.34 oz/lb.

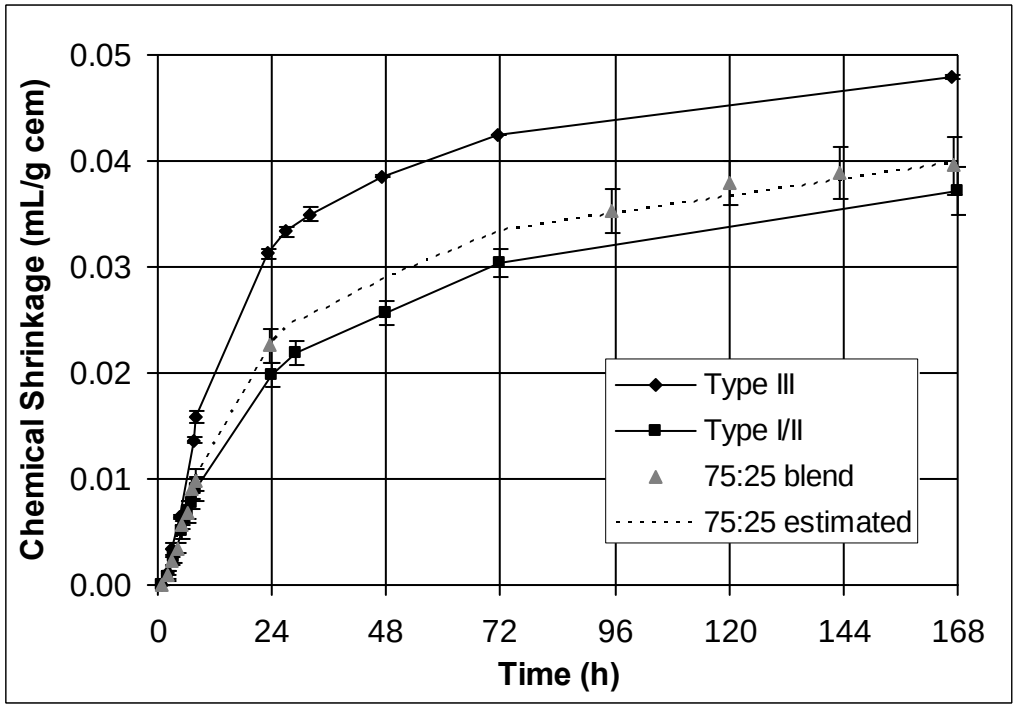

Figure 6. Chemical shrinkage results for the Type I/II and III *w/c* = 0.4 cement pastes and results for the 75:25 *w/c* = 0.4 blend, both as measured and as predicted by applying the law of mixtures. Error bars indicate ± one standard deviation for three replicate specimens for each cement paste. 1 mL/g = 15.34 oz/lb.

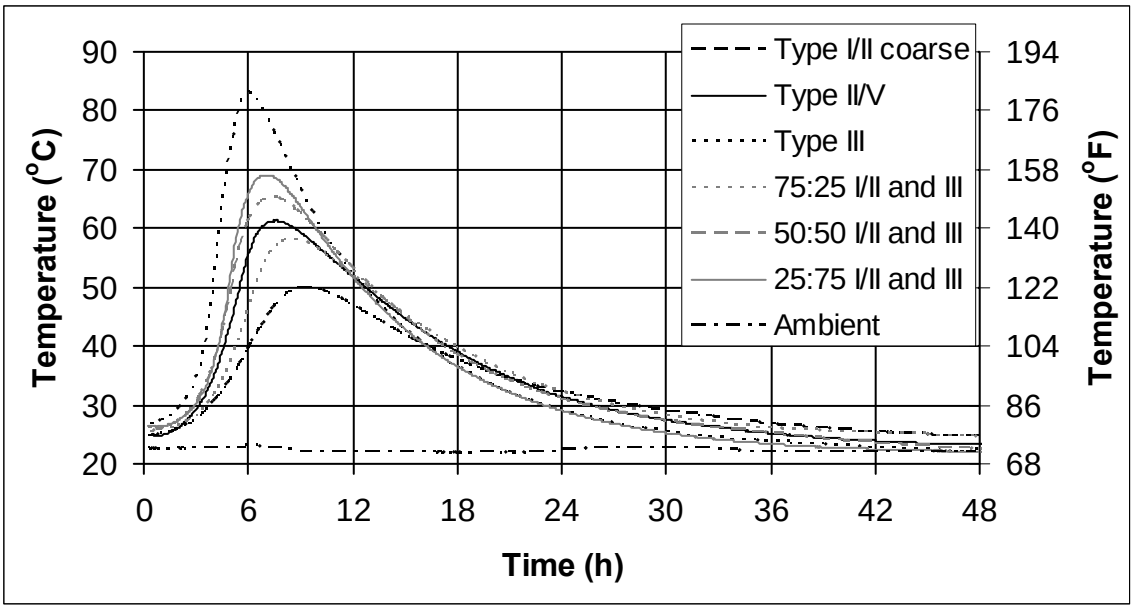

Figure 7. Semi-adiabatic temperature vs. time for the six *w/c* = 0.4 cement pastes.

Table 3. Maximum temperatures measured during semi-adiabatic testing for the 6 cement pastes.

Cement Paste	Measured Maximum Temperature	Predicted Maximum Temperature	Difference (%)
Type I/II coarse	49.9 ºC (121.8 ºF)		
Type II/V	61.3 ºC (142.3 ºF)		
Type III	83.1 ºC (181.6 ºF)		
75:25 I/II and III	58.2 ºC (136.8 ºF)	58.2 ºC (136.8 ºF)	0.1 %
50:50 I/II and III	65.2 ºC (149.4 ºF)	66.5 ºC (151.7 ºF)	1.9 %
25:75 I/II and III	69.1 ºC (156.4 ºF)	74.8 ºC (166.6 ºF)	8.3 %

Table 4. Time of maximum temperature during semi-adiabatic testing for the 6 cement pastes.

Cement Paste	Measured Max Time	Predicted Max Time	Difference (%)
Type I/II coarse	9.2 h		
Type II/V	7.46 h		
Type III	6.03 h		
75:25 I/II and III	8.54 h	8.41 h	-1.6 %
50:50 I/II and III	7.46 h	7.62 h	2.1 %
25:75 I/II and III	7.02 h	6.82 h	-2.8 %

temperature and the time at which it is achieved for the three cement blends are well predicted by applying the law of mixtures to the values measured for the Type I/II and Type III cement pastes. In general, the prediction error is only a few percent, with the exception of the maximum temperature achieved for the 25:75 blend, where it is about 8 %.

The 50:50 blend and the Type II/V cement both exhibit their maximum temperature at an age of 7.46 h, but the temperature produced at this time is higher for the 50:50 blend, perhaps

due to it containing a greater fraction of cement particles smaller than 10 μm when compared to the Type II/V initial cement (Figure 1).

Setting Time (Vicat)

The setting time results for the three initial cements and the three blends are provided in Figure 8. The initial and final setting times as determined from the Vicat needle penetration measurements are summarized in Tables 5 and 6, respectively. For the three initial cements, the setting order is as would generally be expected with finer cements achieving both initial and final set at earlier times, due to their enhanced hydration rates, which for this clinker overwhelm the fact that it may take slightly more hydration to achieve set in a finer cement due to the increased number of particle-to-particle connections (bridges) that may be required.[5] While the results for the three blends do fall between those of their Type I/II and Type III components, it is seen in Tables 5 and 6 that the law of mixtures doesn't accurately predict their initial and final setting times. There are at least two contributions that prevent the law of mixtures from making an accurate prediction in this case. First, at early ages (less than 5 h), degree of hydration is not linear with time (see Figure 6), so that even if the degree of hydration is well predicted by the law of mixtures (as it is in Figures 3 and 6), the time at which a specific degree of hydration is reached may not be accurately predicted. Second, in addition to depending on hydration rates, setting also depends on establishing particle-to-particle contacts, and it was shown in Figure 2 that particle spacing for the blends is not predicted precisely by the law of mixtures. Due to these effects, the errors in setting time predictions are on average greater than the single laboratory precisions quoted for the ASTM C191 standard method,[9] particularly for initial setting times. Conversely, as shown in Tables 5 and 6, the experimental results for the two replicate specimens for each of the 6 pastes generally exhibited a variability well below these single laboratory precision values for normal consistency pastes (12 min and 20 min for initial and final setting, respectively).

The influence of HRWRA dosage on the setting times of the *w/c* = 0.4 Type III cement pastes is shown in Figure 9. While minimal retardation was observed in the isothermal heat flow curves for these four cement pastes in Figure 4, the setting times are seen to vary by up to 2 h in Figure 9. As the HRWRA achieves better dispersion of the cement particles, more hydration (time) will be required to build the bridges between them necessary to cause setting of the paste. This data set highlights the inherent difficulty in utilizing isothermal calorimetry (a measure of chemical reaction or degree of hydration) to estimate setting times (a physical process influenced by both degree of hydration and particle spacing). In addition to not functioning in pastes with various concentrations of HRWRA in this study, it has previously been demonstrated that for pastes with different *w/c*, isothermal calorimetry curves may overlap one another, while considerable differences are observed in their initial and final setting times.[16]

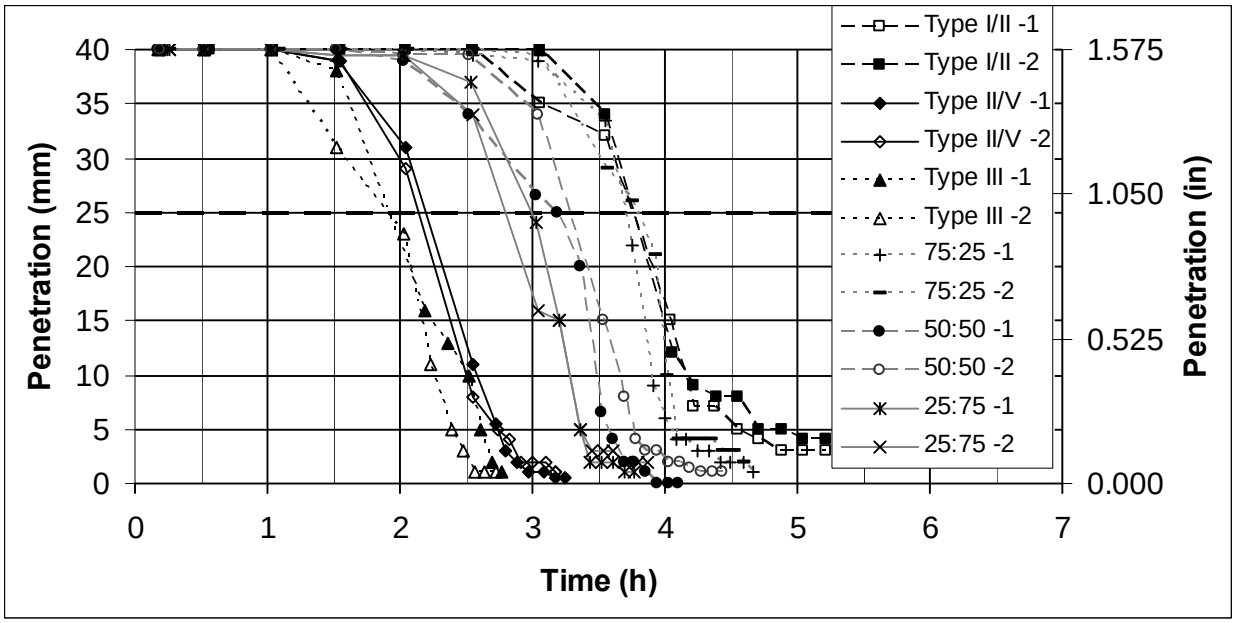

Figure 8. Setting time results for *w/c* = 0.4 cement pastes for the three initial cements and the three blends. Dashed line at a penetration of 25 mm (1 in) indicates initial set. Two replicate measurements from the same batch are shown for each paste to provide an indication of variability.

Table 5. Initial setting times for *w/c* = 0.4 cement pastes as measured by Vicat needle penetration.

Paste	Rep. 1	Rep. 2	Mean setting time	Predicted setting time	Difference
Type I/II coarse	3.75 h	3.76 h	3.76 h		
Type II/V	2.19 h	2.14 h	2.17 h		
Type III	1.92 h	1.91 h	1.92 h		
25:75 blend	2.99 h	2.79 h	2.89 h	2.38 h	30.9 min
50:50 blend	3.19 h	3.27 h	3.23 h	2.84 h	23.7 min
75:25 blend	3.7 h	3.79 h	3.75 h	3.30 h	27 min

Table 6. Final setting times for *w/c* = 0.4 cement pastes as measured by Vicat needle penetration.

Paste	Rep. 1	Rep. 2	Mean setting time	Predicted setting time	Difference
Type I/II coarse	4.88 h	5.05 h	4.97 h		
Type II/V	3.17 h	3.18 h	3.18 h		
Type III	2.77 h	2.56 h	2.67 h		
25:75 blend	3.69 h	3.7 h	3.7 h	3.24 h	27.3 min
50:50 blend	3.94 h	4.27 h	4.11 h	3.82 h	17.4 min
75:25 blend	4.67 h	4.6 h	4.64 h	4.39 h	14.7 min

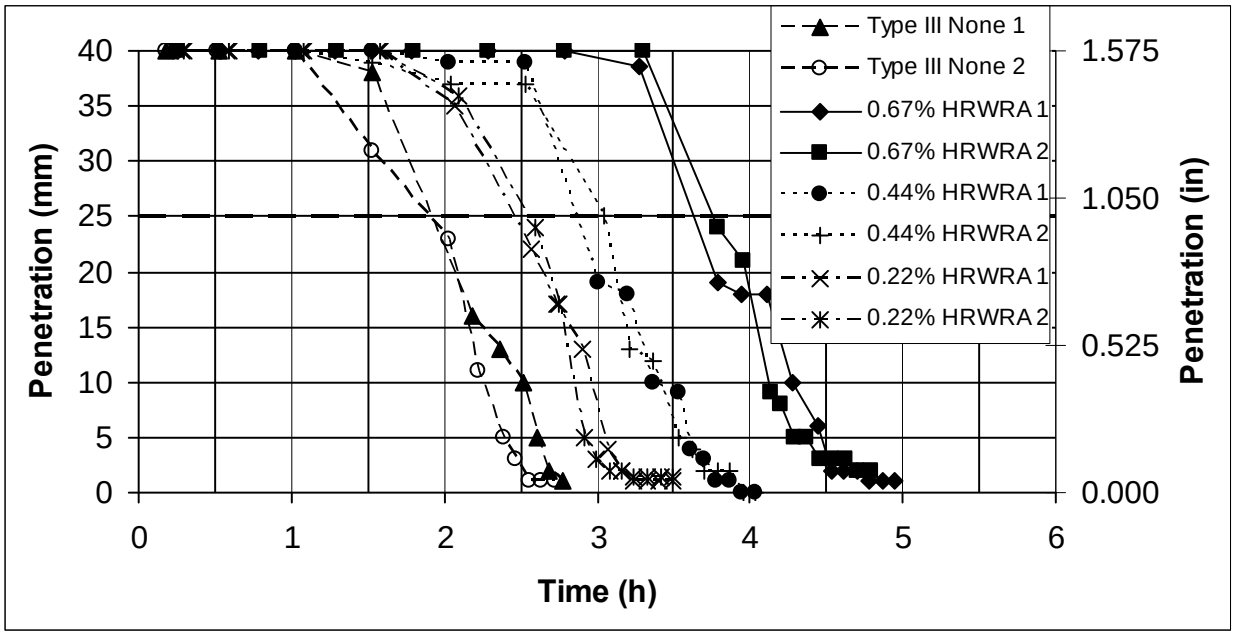

Figure 9. Setting time results for *w/c* = 0.4 Type III cement pastes with various HRWRA addition levels by mass of cement. Dashed line at a penetration of 25 mm (1 in) indicates initial set. Two replicate measurements from the same batch are shown for each paste to provide an indication of variability.

Mortars

Isothermal Calorimetry

The isothermal calorimetry heat flow curves for the first 24 h of hydration for the various mortars are provided in Figure 10. While the HRWRA exhibited minimal retardation in the pastes (above), it produced a significant (2 h or more) retardation in all mortar mixtures into which it was admixed. Since some of the mortars contain HRWRA and others do not, a direct comparison of the heat release curves predicted by the law of mixtures to those measured for the blends, as was performed in Figure 3 for the pastes (all without HRWRA), is not straightforward due to this retardation. Instead, for the blended mortars, the predicted cumulative heat release after various hydration periods (1 d, 3 d, and 7 d) has been computed. These results are presented in Table 7. The law of mixtures is seen to produce reasonable estimates for the cumulative heat release of the blends when the two endpoint components are considered to be the Type I/II and (Type III with HRWRA) mortars. For the 50:50 blend, the predictions are in better agreement with the measured values for the mortar prepared **with** HRWRA than for the one that contained no admixtures, as might be expected since the prediction was made using the Type I/II cement without HRWRA and the Type III cement **with** HRWRA as endpoints. The results in Table 7 imply that for these mortars, the degree of hydration of the blends is adequately predicted by the law of mixtures despite significant differences in their early-age (12 h) hydration, as illustrated in Figure 10. While the shapes of the heat flow curves in Figure 10 are quite different, their integrals for the first 24 h, as quantified by the 1 d heat release values in Table 7, vary in a consistent and predictable fashion.

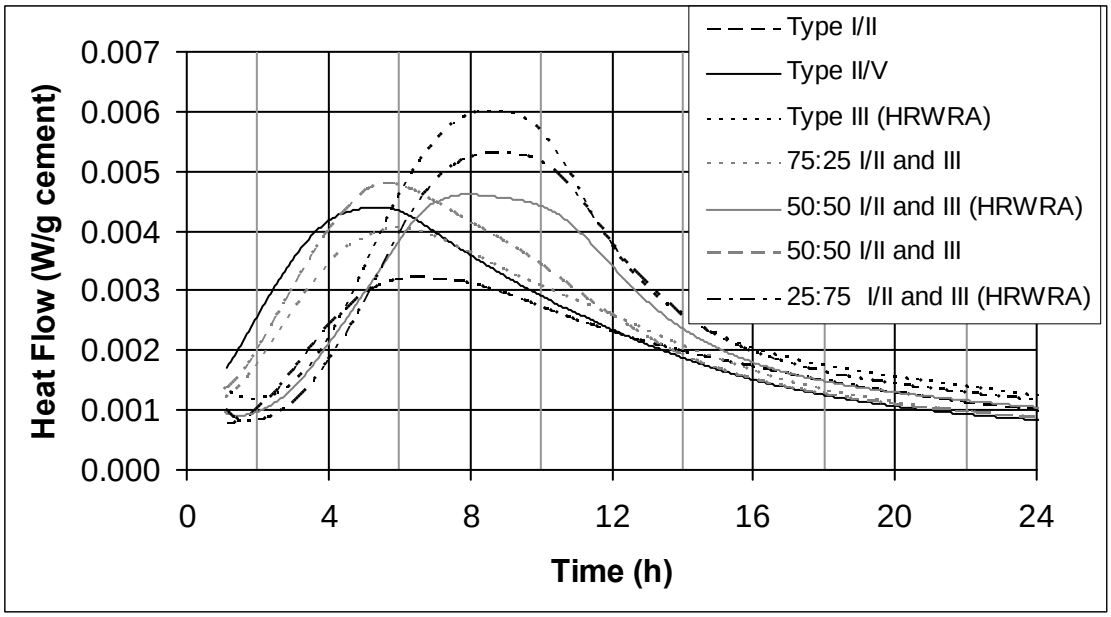

Figure 10. Isothermal calorimetry results out to 24 h for *w/c* = 0.4 mortars based on the three initial cements and the blends of the Type I/II and Type III cements. 1 W/g = 1548 Btu/(h·lb).

Table 7. Cumulative heat release (J/ g cement) for the various mortars and predictions based on the law of mixtures. (1 J/g = 0.43 Btu/lb)

Mortar	**1 d**	**Pred. 1 d (difference %)**	**3 d**	**Pred. 3 d (difference %)**	**7 d**	**Pred 7 d (difference %)**
Type I/II	165 J/g		254 J/g		301 J/g	
Type II/V	194 J/g		275 J/g		309 J/g	
Type III (HRWRA)	238 J/g		323 J/g		348 J/g	
75:25 I/II & III	186 J/g	183 J/g (-1.4 %)	266 J/g	271 J/g (2.0 %)	305 J/g	313 J/g (2.6 %)
50:50 I/II & III	216 J/g	202 J/g (-6.6 %)	301 J/g	288 J/g (-4.3 %)	332 J/g	324 J/g (-2.4 %)
50:50 I/II & III (HRWRA)	202 J/g	202 J/g (-0.2 %)	286 J/g	288 J/g (0.86 %)	316 J/g	324 J/g (2.6 %)
25:75 I/II & III (HRWRA)	220 J/g	220.03 (-0.2 %)	307 J/g	306 J/g (-0.45 %)	334 J/g	336 J/g (0.66 %)

Semi-adiabatic Calorimetry

The semi-adiabatic testing results for the mortars are summarized in Figure 11 and Table 8. The retarding influence of the HRWRA on hydration in the mortars is clearly observed in the results in Figure 12, where those mortars containing HRWRA exhibit a shift of their peak

temperature to later times, consistent with the isothermal calorimetry results in Figure 10. Still, as illustrated in Table 8, the law of mixtures provides reasonable predictions for the maximum achieved temperatures in the blends based on the values measured on the Type I/II and (Type III with HRWRA) component mortars. Conversely, unlike the cement paste data presented in Table 4, for the mortars, the time of maximum temperature ranged between 9.7 h and 11.4 h in a non-systematic manner and was not well predicted by the law of mixtures, as the influence of cement PSD on these times was confounded by the strong retarding influence of the HRWRA, when present in the mortar mixtures.

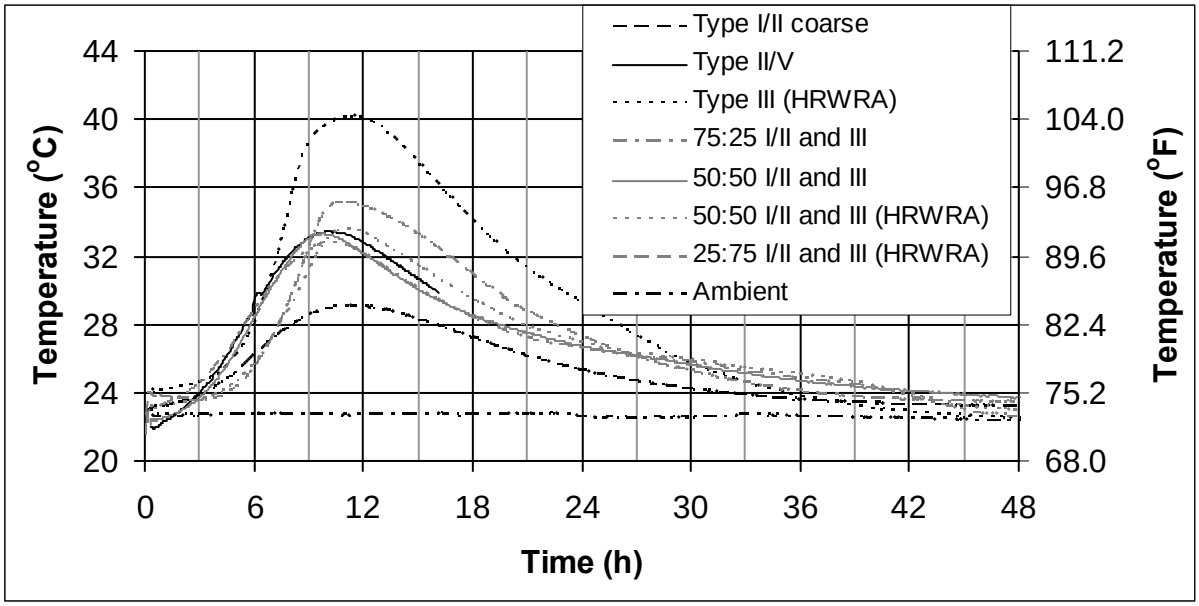

Figure 11. Semi-adiabatic temperature vs. time for mortars.

Table 8. Maximum temperatures measured during semi-adiabatic testing for mortars.

Mortar	Measured Maximum Temperature	Predicted Maximum Temperature	Difference (%)
Type I/II coarse	29.1 ºC (84.4 ºF)		
Type II/V	33.4 ºC (92.1 ºF)		
Type III (HRWRA)	40.2 ºC (104.4 ºF)		
75:25 I/II and III	32.8 ºC (91.0 ºF)	31.9 ºC (89.4 ºF)	-2.8 %
50:50 I/II and III	33.3 ºC (91.9 ºF)	34.7 ºC (94.5 ºF)	4.1 %
50:50 I/II and III (HRWRA)	33.6 ºC (92.5 ºF)	34.7 ºC (94.5 ºF)	3.2 %
25:75 I/II and III (HRWRA)	35.2 ºC (95.4 ºF)	37.5 ºC (99.5 ºF)	6.5 %

Compressive Strength

The mortar cube compressive strength results are provided in Table 9. The graph in Figure 12 provides both an indication of the measurement variability and the ability of the law of mixtures to adequately predict the compressive strengths. In general, the predictive capability of the law of mixtures is adequate as the predictions generally lie within one standard deviation (based on three measured replicates) of the measured mean values for the mortars based on the

cement blends. Further, with the exception of the 50:50 blend without HRWRA, all of the predictions are within 10 % of their corresponding measured value. The addition of the HRWRA to the 50:50 blend is seen to increase measured compressive strengths at all ages, perhaps due to better compaction within the cube molds and/or better dispersion of the cement particles.

Table 9. Compressive strengths vs. age for the various *w/c* = 0.4 mortars.

Mortar	**1 d (MPa/psi)**	**3 d (MPa/psi)**	**7d (MPa/psi)**	**28 d (MPa/psi)**	**91 d (MPa/psi)**
Type I/II	15.7 MPa 2280 psi	32.6 MPa 4720 psi	43.2 MPa 6270 psi	54.7 MPa 7930 psi	67.4 MPa 9800 psi
Type II/V	28.7 MPa 4160 psi	48.5 MPa 7040 psi	55.4 MPa 8040 psi	66.2 MPa 9600 psi	77.9 MPa 11300 psi
Type III (HRWRA)	51.7 MPa 7500 psi	70.4 MPa 10210 psi	80.5 MPa 11670 psi	86.8 MPa 12590 psi	98.0 MPa 14200 psi
75:25 I/II & III	24.0 MPa 3480 psi	40.4 MPa 5850 psi	50.0 MPa 7250 psi	61.2 MPa 8880 psi	71.2 MPa 10330 psi
50:50 I/II & III	29.7 MPa 4310 psi	46.4 MPa 6720 psi	54.4 MPa 7890 psi	65.9 MPa 9550 psi	73.3 MPa 10630 psi
50:50 I/II & III (HRWRA)	31.0 MPa 4490 psi	50.8 MPa 7360 psi	61.0 MPa 8840 psi	74.4 MPa 10780 psi	80.5 MPa 11680 psi
25:75 I/II & III (HRWRA)	39.0 MPa 5650 psi	58.9 MPa 8540 psi	68.5 MPa 9930 psi	80.1 MPa 11620 psi	93.5 MPa 13560 psi

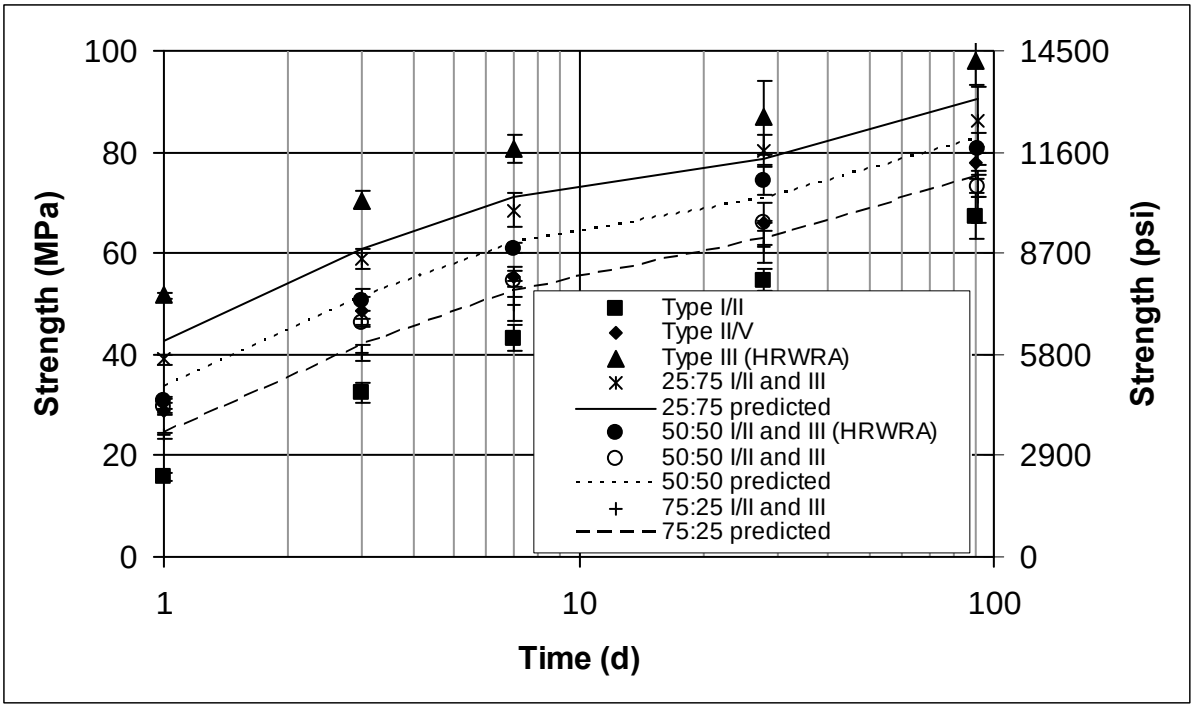

Figure 12. Measured and predicted (law of mixtures) compressive strengths vs. time for the various mortar mixtures. Error bars for each symbol indicate ± one standard deviation for three replicate specimens for each mortar at each age.

In Table 9, 28-d compressive strengths are seen to vary from 54.7 MPa (7930 psi) to 86.8 MPa (12590 psi) for the five mortars comprising the three blends and the two pure blending component cements. Thus, a range that encompasses over a 50 % increase in compressive strength is obtained simply by controlling the cement PSD. At 1 d, these strengths encompass over a 300 % increase in compressive strength. These results imply that a wide range of compressive strengths can be readily produced by the judicious blending of two cements of widely different finenesses.

The correlation between heat release and compressive strength is explored in Figure 13 that plots the two variables. For any given age, a generally linear relationship is observed between compressive strength and heat release (a measure of degree of hydration). It should be noted that for each age in Figure 13, the individual data point outlier that falls well below the general trend (line) corresponds to the 50:50 blend of the Type I/II and Type III cements with no chemical admixtures. As mentioned previously, these "lower" strengths could be due to difficulties in properly compacting that particular mortar into its cube molds. The results in Figure 13 also indicate that for equivalent heat releases, lower compressive strengths will be obtained for coarser cements, likely due to their increased initial interparticle spacing (Figure 2).

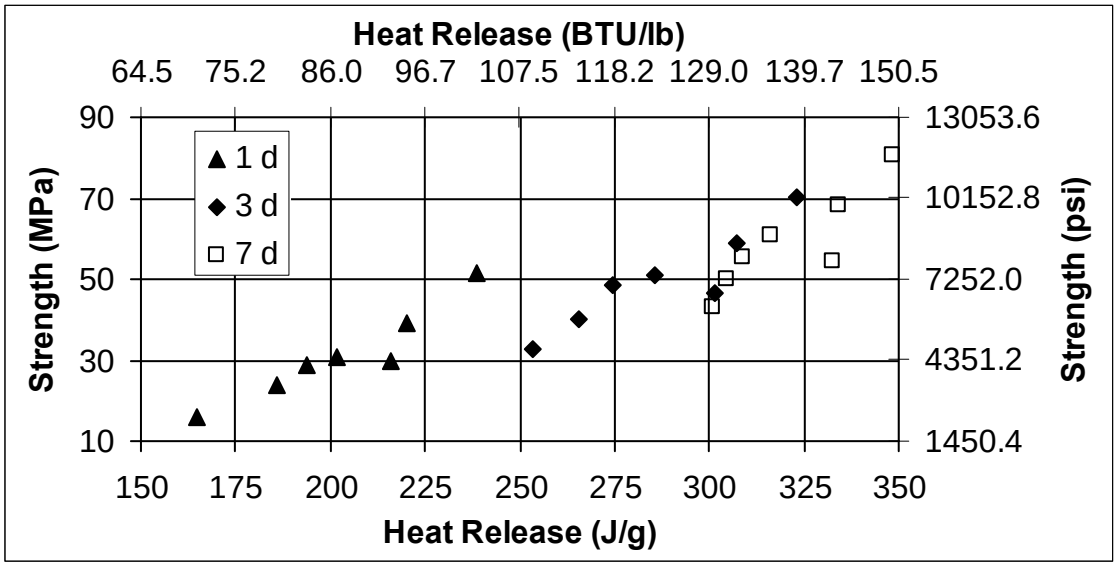

Figure 13. Compressive strength vs. heat release at 3 different ages for the mortars examined in this study. For each age, data points from left to right correspond to Type I/II, 75:25 blend, Type II/V, 50:50 blend with HRWRA, 50:50 blend with no HRWRA, 25:75 blend, and Type III cements, respectively.

Autogenous Deformation

The early-age (autogenous) deformation results for the mortars are provided in Figure 14. All of the mixtures experienced a significant later age shrinkage, with the finer PSD mixtures exhibiting this shrinkage from the time of set and the coarser PSD mixtures first exhibiting an expansion, followed by the shrinkage. Recently, Cusson has advocated the utilization of the (net) difference between the maximum (peak) and minimum (achieved post peak) deformations achieved during the first 7 d of curing as an effective measure of the risk of cracking in a

concrete structure, as a concrete typically reaches a zero-stress state sometime after the peak (expansion) is achieved, but prior to the autogenous deformation returning to zero (or achieving its minimum value).[17] Beyond this zero-stress time, tensile stresses develop and build under restrained conditions and may ultimately lead to early-age cracking if the tensile strength of the concrete is exceeded at any time.[17] For the mortars examined in this study, these values of (ε_{min}-ε_{max}) at 7 d are summarized in Table 10. For the three initial cements, the net deformation increases rapidly with increasing fineness. The results for the blends lie in between those of the component mortars, but are not accurately predicted by the simple law of mixtures. The stresses generated within the sealed hydrating mortars are inversely proportional to the size of the pores being emptied by chemical shrinkage and its accompanying self-desiccation. Since the resulting deformation will depend both on hydration (rates) and interparticle spacing as was also the case for setting times, once again, the law of mixtures is inadequate for predicting performance.

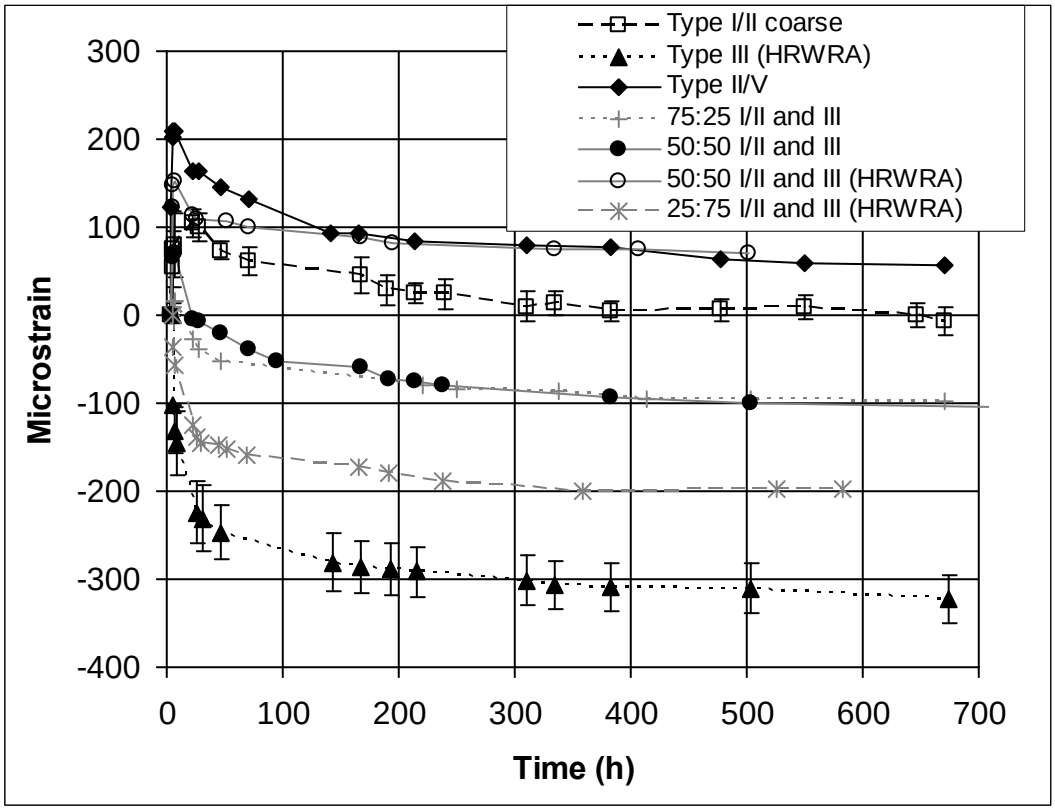

Figure 14. Autogenous deformation results for the various mortar mixtures. Error bars indicating ± one standard deviation for three replicate specimens are provided for two of the data sets to provide an indication of variability.

The results for the 50:50 blend with and without the HRWRA in Figure 14 and Table 10 suggest that the extra dispersion provided by the HRWRA increases the early-age expansion and significantly reduces the net deformation achieved after 7 d of sealed curing. The increased interparticle distances and the reduced hydration rates (retardation) in mortars are two characteristics imparted by the addition of the HRWRA that could contribute to a beneficial reduction in autogenous shrinkage.

Table 10. Measured and predicted net autogenous deformations at 7 d for the mortar mixtures.

Mortar	$(\varepsilon_{min}-\varepsilon_{max})$ – 7 d	Predicted	Difference (microstrain)
Type I/II	-58		
Type II/V	-117		
Type III (HRWRA)	-286		
75:25 I/II and III	-84	-115	-31
50:50 I/II and III	-131	-172	-41
50:50 I/II and III (HRWRA)	-71	-172	-101
25:75 I/II and III (HRWRA)	-172	-229	-57

The Type II/V cement mortar exhibited a net deformation at 7 d that lies between the two 50:50 blends (with and without HRWRA). However, in Figure 14, it is observed that the early-age expansion for the Type II/V mortar was the greatest observed in this study. It is possible that the PSD of the gypsum in the Type II/V mortar is finer than that obtained in the 50:50 blend (since the softer gypsum was interground with the harder cement in the former case while in the latter case, the gypsum coming from the coarse component of the blend may have not been ground as finely), leading to an increase in aluminate hydration and ettringite formation at early ages, with an accompanying increase in expansion.[18]

Summary of Influence of Cement Fineness on Paste and Mortar Properties

While not the primary purpose of this study, this data set also provides a quantitative examination of the influence of cement fineness on properties of cement pastes and mortars, as summarized in Table 11. Clearly, cement fineness plays a major role in establishing the properties of a cement paste or mortar, with some properties varying by over a factor of three for the three levels of fineness examined in this study. A move towards finer cements would be expected to be accompanied by increased strengths (particularly at early ages), a reduced setting times, and concurrent increases in early-age temperature rise and autogenous deformation. These effects should be appropriately considered when selecting the fineness of cement to employ for a particular construction project.

Conclusions

The controlled blending of a coarse and a fine cement provides the possibility to produce performance properties that span a large range of values. Isothermal heat release, semi-adiabatic temperature rise, setting time, compressive strength, and autogenous deformation all change significantly with a change in the cement PSD. The results of this study have indicated that the degree of hydration for cements produced by blending two different finenesses can be adequately predicted from the hydration characteristics of the two components by applying a simple law of mixtures. Because the law of mixtures works well for predicting degree of hydration of the blends, properties of the blended pastes and mortars that are basically proportional to degree of hydration, such as heat of hydration, chemical shrinkage, and even compressive strength, can also be accurately predicted by applying the law of mixtures. Conversely, properties such as autogenous deformation and setting that are dependent on both degree of hydration and interparticle spacing were not accurately predicted by the simple law of mixtures in this study.

In these cases, experimental measurements of the setting and early-age deformation properties of the blends must be completed or more complex models applied to quantify their performance. This study has demonstrated the potential of engineering the performance of cement-based materials by controlling the PSD of the starting hydraulic binder.

Table 11. Paste and mortar properties for the cements of three different finenesses.

Property	**Type I/II (302 m^2/kg)**	**Type II/V(387 m^2/kg)**	**Type I/II (643 m^2/kg)**
Paste- initial set	3.76 h	2.17 h	1.92 h
Paste – final set	4.97 h	3.18 h	2.67 h
Mortar – 1 d heat release	165 J/g	194 J/g	238 J/g
Mortar – 7 d heat release	254 J/g	275 J/g	323 J/g
Mortar – Semi-adiabatic maximum temperature	29.1 ºC (84.4 ºF)	33.4 ºC (92.1 ºF)	40.2 ºC (104.4 ºF)
Mortar – 1 d strength	15.7 MPa (2280 psi)	28.7 MPa (4160 psi)	51.7 MPa (7500 psi)
Mortar – 28 d strength	54.7 MPa (7930 psi)	66.2 MPa (9600 psi)	86.8 MPa (12590 psi)
Mortar – 7 d net autogenous shrinkage	-58 με	-117 με	-286 με

Acknowledgements

The author would like to thank the Lehigh Cement Corporation (Redding, CA plant) for providing the three cements used in this study and W.R. Grace & Co.- Conn. for supplying the water-reducing admixture. He would also like to thank his colleagues in the Building and Fire Research Laboratory: Dr. Chiara Ferraris, Mr. Max Peltz, and Mr. John Winpigler for their assistance with the experimental program.

REFERENCES

1. Frigione, G., and Marra, S., "Relationship Between Particle Size Distribution and Compressive Strength in Portland Cement," *Cement and Concrete Research*, V. 6, 1976, pp.113-127.
2. Osbaeck, B., and Johansen, V., "Particle Size Distribution and Rate of Strength Development of Portland Cement," *Journal of the American Ceramic Society*, V. 72, No. 2, 1989, pp. 197-201.
3. Wakasugi, S., Sakai, K., Shimobayashi, S., and Watanabe, H., "Properties of Concrete using Belite-Based Cement with Different Finenesses," Proceedings of Concrete under Severe Conditions 2 Environment and Loading, V. 3, Ed. O.E. Gjorv, K. Sakai, and N. Banthia, et al., E&FN Spon, 1998, pp. 2161-2169.
4. ASTM C 150-07, "Standard Specification for Portland Cement," ASTM International, West Conshohocken, PA, 2007.
5. Bentz, D.P., Sant, G., and Weiss, W.J., "Early-Age Properties of Cement-Based Materials: I. Influence of Cement Fineness," *ASCE Journal of Materials in Civil Engineering*, V. 20, No. 7, 2008, pp. 502-508.
6. ASTM C 778-05, "Standard Specification for Standard Sand," ASTM International, West Conshohocken, PA, 2005.
7. Bentz, D.P., and Turpin, R., "Potential Applications of Phase Change Materials in Concrete Technology," *Cement and Concrete Composites*, V. 29, No. 7, 2007, pp. 527-532.
8. ASTM C 1608-05, "Standard Test Method for Chemical Shrinkage of Hydraulic Cement Paste," ASTM International, West Conshohocken, PA, 2005.
9. ASTM C 191-99, "Standard Test Method for Time of Setting of Hydraulic Cement by Vicat Needle," ASTM International, West Conshohocken, PA, 1999.
10. ASTM C 109/C 109 M-99 , "Standard Test Method for Compressive Strength of Hydraulic Cement Mortars (Using 2-in. or [50-mm] Cube Specimens)," ASTM International, West Conshohocken, PA, 1999.
11. Jensen, O.M., and Hansen, P.F., "A Dilatometer for Measuring Autogenous Deformation in Hardening Portland Cement Paste," *Materials and Structures*, V. 28, 1995, pp. 406-409.
12. Bentz, D.P., and Aitcin, P.-C., "The Hidden Meaning of Water-to-Cement Ratio," *Concrete International*, V. 30, No. 5, 2008, pp. 51-54.
13. Verbeck, G.J., and Foster, C.W., "Long-Time Study of Cement Performance in Concrete, Chapter 6 – The Heats of Hydration of the Cements," Proceedings of ASTM, V. 50, No. 150, 1950, pp. 1235-1262.
14. Powers, T.C., "Adsorption of Water by Portland Cement Paste during the Hardening Process," *Industrial and Engineering Chemistry*, V. 27, 1935, pp. 790-794.
15. Bentz, D.P., "Three-Dimensional Computer Simulation of Portland Cement Hydration and Microstructure Development," *Journal of the American Ceramic Society*, V. 80, No. 1, 1997, pp. 3-21.
16. Bentz, D.P., Peltz, M.A., and Winpigler, J., "Early-Age Properties of Cement-Based Materials: II. Influence of Water-to-Cement Ratio," submitted to *ASCE Journal of Materials in Civil Engineering*, 2008.
17. Cusson, D., "Effect of Blended Cements on Efficiency of Internal Curing of HPC," ACI-SP 256, Internal Curing of High-Performance Concretes: Laboratory and Field Experiences, American Concrete Institute, Farmington Hills, MI, 2008, pp. 105-120.

18. Bentz, D.P., and Peltz, M.A., "Reducing Thermal and Autogenous Shrinkage Contributions to Early-Age Cracking," *ACI Materials Journal*, V. 105, No. 4, 2008, pp. 414-420.